Lab 2 Report

Kalie Knecht

December 22, 2022

Introduction

When radiation interacts in a semiconductor detector, it generates charge carriers called holes and electrons which move through the detector volume toward their respective electrodes. The signals from a semiconductor detector arise from the motion of these charge carriers. The output pulse from a detector begins as soon as the charge carriers start their motion. The time profile of the signal can be used to determine timing properties, as well as interaction locations within the detector volume. This has important implications in fields such as radiation imaging, where the precise interaction location is a crucial ingredient in reconstructing where the incident radiation originated. Knowing interaction locations can also be useful for filtering out events that arise in regions of the detector susceptible to strong charge trapping, resulting in higher quality spectral analysis.

In this experiment, we perform pulse shape analysis on signals generated from a cylindrical High Purity Germanium (HPGe) detector. We build on the pulse processing techniques developed in experiment 1, and perform additional analysis on the pulses to correlate different pulse shapes with spectral features.

Methods

0.1 Detector Acquisition System

In this experiment, we used a liquid nitrogen cooled co-axial HPGe detector biased at 3200 V. The HPGe detector is connected to a pre-amplifer, which is housed within the detector cryostat to reduce noise. The pre-amplifer output cable is connected to a Struck Innovation Systems (SIS) 16 Channel VME Digitizer card, which sends raw digitized pulse waveforms to a computer via an ethernet cable. The *Ethernet Data Aquisition Code for SIS3316 250MHz Digitizers data acquisition software* package from the BeARING github [1] is used to aquire data from the detector with the digitizer. The data acquisition parameters are customizable through a JSON configuration file. The same configuration from experiment 1 was used in this laboratory.

A trapezoidal shaping filter described by Cooper [4], implemented in python by Jaewon Lee, is applied to the raw pre-amplifier pulses output from the SIS digitizer. The tau, peaking time, and gap time used for filtering in experiment 1 are also used in this experiment.

Co-60, Ba-133, and Cs-137 sources were previously used to find the energy and energy resolution calibration of the detector. The peak energies, activities, and associated isotopes of the calibration sources are summarized in Table 1. The calibrations generated in experiment 1 are also used for this experiment. The Cs-137 check source that was used to calibrate the detector was also used for this experiment. The source was placed at a 25 cm source-to-detector distance on axis with the detector and data was collected for 10 minutes.

Isotope	Activity 10/28/22 [μCi]	Energy [kev]	Intensity [%]
Ba-133	5.26	383.9	8.94
Cs-137	8.21	661.7	85.1
Co-60	2.46	1173.2	99.85
Co-60	2.46	1332.5	99.98

Table 1: Check sources used in the laboratory with their activity and associated gamma-ray energies and intensities from [3]

0.2 Peak-to-Compton (PC) ratio

The peak-to-Compton ratio is an index of detector performance which measures the combined effects of detector energy resolution and photofraction. A large PC ratio represents a spectrum with a suppressed Compton continuum. The PC ratio is defined as:

$$PC = \frac{\text{count in highest photopeak channel}}{\text{count in a typical channel of the Compton continuum associated with that peak}} \quad (1)$$

The sample of the continuum is to be taken in the relatively flat portion of the distribution lying to the left of the rise toward the Compton edge. To avoid selecting a Compton bin with 0 counts, the mean counts in a sample of 10 bins to the left of the Compton edge are used as the count in a typical channel of the Compton continuum. The count in the highest photopeak channel is taken from the peak found in the peak finding algorithm developed in experiment 1.

0.3 Peak-to-total (PT) ratio

Another index of detector performance is the PT ratio. A large PT ratio represents a large fraction of photopeak events. The PT ratio is defined as:

$$PT = \frac{\text{count in highest photopeak channel}}{\text{count in all channels}} \quad (2)$$

The count in all channels is found as the sum of all counts in the spectrum, while the count in highest photopeak channel is the same as what is found for the PC ratio.

0.4 Pulse Shape Analysis

The signal generated by a semiconductor detector is a result of the induced charge on electrodes as charge carriers move along the electric field in the detector. The shape of the leading edge of pulses from HPGe detectors depends on the position where the gamma-ray interaction occured within the active detector volume [5], as shown in Fig. 1. Therefore, the radial position of the gamma-ray interaction may be inferred through the resulting pulse shape. Position information of radiation interactions is required for imaging applications.

0.4.1 Rise Time

The shape of the rising edge of a pulse can be defined in terms of its rise time. For this experiment, the rise time is calculated as the time it takes for signal to rise from 10% of the maximmum to 90% of the maximum.

$$\text{Rise Time} = t_{90} - t_{10} \quad (3)$$

where t_{90} is the time for signal to rise to 90% of maximum and t_{10} is the time for signal to rise to 10% of maximum.

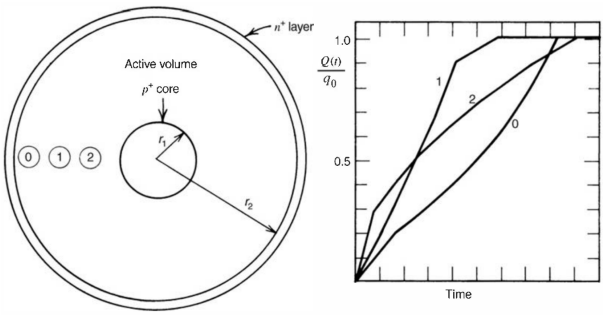

Figure 1: Different interaction locations within the HPGe detector result in different pulse shapes, figure 12.13 from [5].

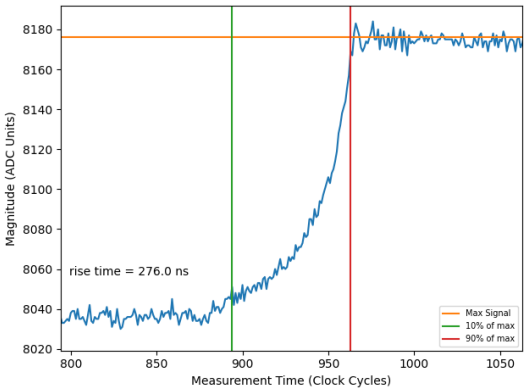

Figure 2: Calculation of rise time, with the maximum signal denoted by orange, t_{90} in red, and t_{10} in green.

To calculate the rise time of the pulses in this experiment, a sample of each waveform around the rising edge is normalized by subtracting the mean baseline amplitude during the pre-trigger delay period. The max signal in this sample is approximated by finding the absolute maximum, and then this value is refined by taking the mean value over a short range of values following the absolute maximum. The time index where 90% and 10% of this maximum value are found, and the difference between them is computed and converted to nanoseconds. Fig. 2 illustrates how the rise time was calculated for a single pulse. The measurement time at the green line, t_{10}, is subtracted from the measurement time at the red line, t_{90}. The time scale is originally in units of clock cycles, with a clock frequency of 250 MHz, so the rise time is converted to nanoseconds by multiplying the time difference by 4.

0.4.2 Event selection filtering

The signal shapes of the waveforms are used to define different event selection filters to improve the PC and PT ratios. To increase these ratios, a higher fraction of events must correspond to full energy depositions within the detector, and a lower fraction of events must correspond to Compton scattering. A lower energy resolution will also improve these ratios because a higher number of counts will be in the highest photopeak channel.

The first filter investigated is extracting 'fast' and 'slow' pulses. A fast pulse is a pulse with a small rise time, and a slow pulse is a pulse with a large rise time. The rise time is found for all events, as described in equation 3, and slow and fast pulses are selected based on their rise times. For this experiment we describe slow pulses as pulses with a rise time greater than or equal to the mean rise time of all events plus the standard deviation in rise times. Fast pulses are pulses with a rise time less than or equal to the mean rise time of all events minus the

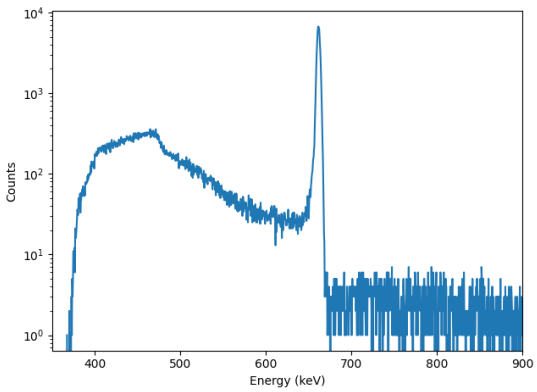

Figure 3: Cs-137 spectrum derived from all waveforms

standard deviation in rise times. A spectrum is generated for fast and slow pulses, and their features and characteristics are compared.

The second approach taken to filter events is k-means clustering [2]. K-means clustering is a method of grouping observations into some number of clusters where each observation belongs to a cluster with the nearest mean. For this experiment, we expect a k-means clustering algorithm to group pulses into clusters of pulses with related shapes, which can be used to filter similar events and perform spectral analysis. To perform k-means clustering, the waveforms are first cropped to a time window around the initial rise and min-max normalized. The *scikit-learn* implementation of the k-means clustering model is then fit to the cleaned waveforms for 2, 3, 4, and 5 clusters.

0.4.3 Multi Interaction events

In this experiment, the pulse shapes are also analyzed to determine which waveforms are multi-site interaction events. In Ge (Z=32) the photoelectric effect is dominant only at gamma-ray energies below about 140 keV. This means that for a 662 keV gamma-ray, it is more likely for full energy events to be comprised of a Compton scatter followed by a photoelectric effect. Therefore, we expect a portion of our photopeak events to be comprised of multi-interaction events. It is possible to determine which events are multi-interaction events based on their pulse shape. We also expect to see multiple interaction events in the Compton valley. The Compton valley sits between the Compton edge and the photopeak, and it represents a portion of events which come from multiple Compton scatters that did not result in a full energy deposition.

Results

0.5 Detector Calibration

The same energy and energy resolution calibration as experiment 1 is used in this experiment. Fig. 3 shows the calibrated energy spectrum obtained with all of the pulses. The PC and PT ratios are determined to be **21.14 +/- 0.07** and **0.045 +/- 0.015** respectively through equations 1 and 2. The goal of event filtering is to downselect all of the waveforms to a portion that will result in a higher PC and PT ratio than that of the full spectrum.

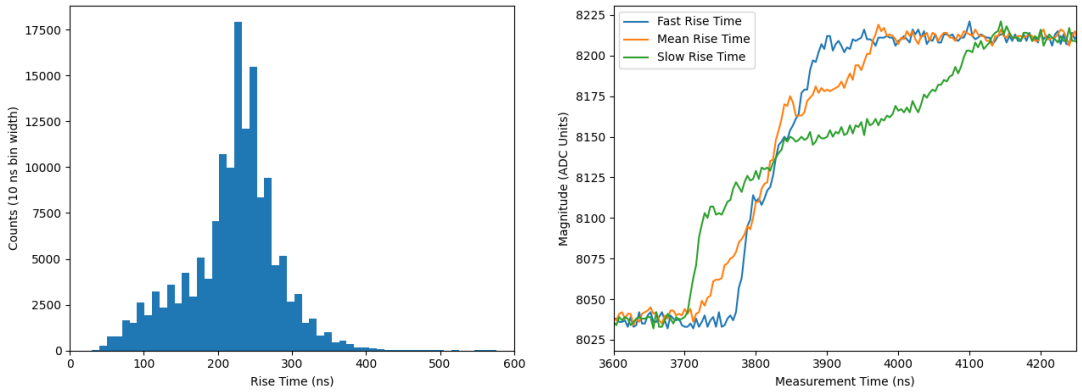

Figure 4: Left: Histogram of rise times for all pulses. Right: Example pulses with fast, slow, and mean rise times.

Dataset	Number of Pulses	Mean Rise Time (ns)	PC Ratio	PT Ratio
Fast Pulses	12,694	93.5 +/- 0.2	23.83 +/- 0.23	**0.050 +/- 0.049**
Slow Pulses	5,201	496.5 +/- 5.1	**49.29 +/- 0.51**	0.047 +/- 0.078
All Pulses	**150,612**	226.3 +/- 0.3	21.14 +/- 0.07	0.045 +/- 0.015

Table 2: Rise time filter impact on PC and PT ratios

0.6 Pulse Shape Analysis

0.7 Rise Time

Equation 3 is used to compute the rise time for all pulses collected. Fig. 4, left shows a histogram of the rise times for all pulses. The mean rise time is 226.3 +/- 0.3 ns. Fig. 4, Right shows example fast and slow pulses, as well as pulse with the mean rise time of 226 ns. Out of 150,612 pulses, we considered 12,694 to be fast and 5,201 to be slow.

0.8 Event Filters

0.8.1 Fast vs. Slow Pulses

The first event filter investigated is filtering out the fast and slow pulses. The fast and slow pulses are each loaded into their own spectra using a previously determined energy calibration. Fig. 5 shows the resulting spectra from fast (left) and slow (right) events. Visual inspection shows that the Compton continuum is suppressed in the slow event spectra obtained, but both spectra show a significant photopeak. Table 2 shows the PC and PT ratios calculated for each of these spectra. Both of these filters result in a larger PC and PT ratio than the full spectrum, however the filters are highly restrictive and result in much fewer counts, which adversely affects energy resolution.

From Fig. 1, slower rise pulses occur closer to the center of the cylindrical detector while faster rise pulses occur closer to the outside of the detector. The suppressed Compton continuum for slow rise pulses could be because those interactions are occurring closer to the center of the HPGe volume, and therefore more likely to deposit all of their energy in the detector volume. Conversely fast rise pulses occur closer to the outer shell of the detector and are therefore more likely to scatter out of the volume, resulting in partial energy deposition.

0.8.2 Result of k-means clustering algorithm with 2 output clusters.

2 clusters

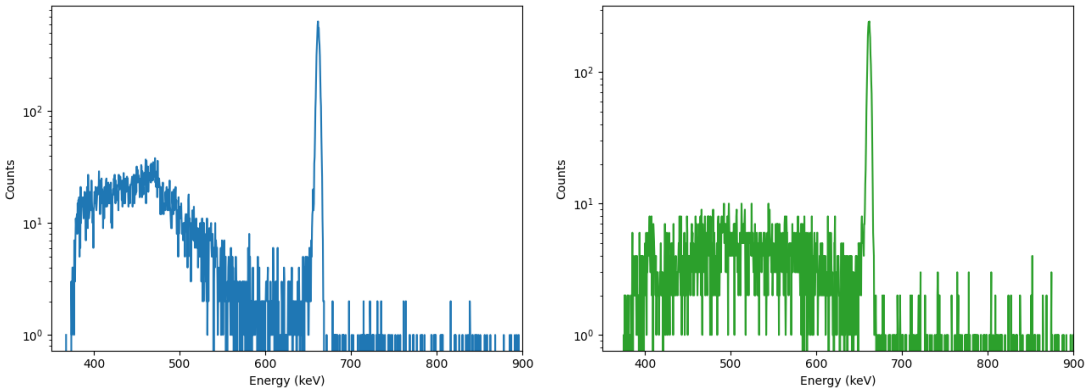

Figure 5: Left: Spectrum of Fast Pulses, Right: Spectrum of Slow Pulses

Cluster	Number of Pulses	Mean Rise Time (ns)	PC Ratio	PT Ratio
0	67,714	229.6 +/- 0.4	0.11 +/- 0.54	0.0001 +/- 0.016
1	84,343	223.7 +/- 0.3	inf	**0.0804 +/- 0.012**
All Pulses	**150,612**	226.3 +/- 0.3	21.138	0.0445

Table 3: PC and PT ratio of k-means clustering algorithm with 2 output clusters.

The first clustering event filter used divides all of the waveforms into two clusters. Fig. 6, top shows a sample of typical pulse shapes of the 2 clusters identified by the k-means clustering algorithm. Fig. 6, bottom shows the resulting spectra from each of these clusters. Cluster 0 appears to be comprised mostly of Compton events with partial energy deposition - the photopeak has less counts than many bins in the Compton continuum. Conversely the cluster 1 spectrum shows a great deal of Compton continuum suppression.

Table 3 shows the PC and PT ratio for each of these clusters, as well as the number of events selected. The PT ratio for Cluster 1 is nearly twice that of the full spectrum. Its PC ratio computation results in a division by 0 because there are no counts lying below the Compton edge.

3 clusters

The next clustering event filter used divides all of the pulses into three clusters. The top left plot in Fig. 7 shows the resulting 3 pulse shapes. Each of the three spectra show a photopeak, but it is the highest in cluster 1. The cluster 1 spectra shows a suppressed Compton continuum - there are no counts below the Compton edge. Cluster 2 and 3 both show more counts in a typical Compton continuum bin than in the photopeak channel, but the cluster 0 continuum shows more counts in the Compton valley, corresponding to events that underwent multiple Compton scatters but did not deposit all of their energy in the detector.

Table 4 shows the mean rise times, PC ratio, and PT ratio of each of the clusters. We can see that the cluster 0 has a relatively fast rise time, cluster 2 has a relatively slow rise time, while cluster 1 has a rise time similar to the mean rise time of all events. As expected from visual inspection of the spectra, Cluster 1 has the largest PT ratio, and the PC ratio cannot be computed due to a lack of counts below the Compton edge.

4 clusters

The next clustering filter used divides the waveforms into four clusters. The top plot in Fig. 8 shows the characteristic pulse shapes of each of the 4 clusters. By visual inspection, the spectra shown in Fig. 8 show that cluster 0 consists of photopeak events with a suppressed Compton continuum. Clusters 1 and 2 mostly consist of Compton events, with their spectra matching the general shape of the spectra in Fig. 7 of clusters 2 and 0 respectively. Similar to cluster 0 of the 3 cluster event filter, we expect cluster 2 to have multi-interaction events due to

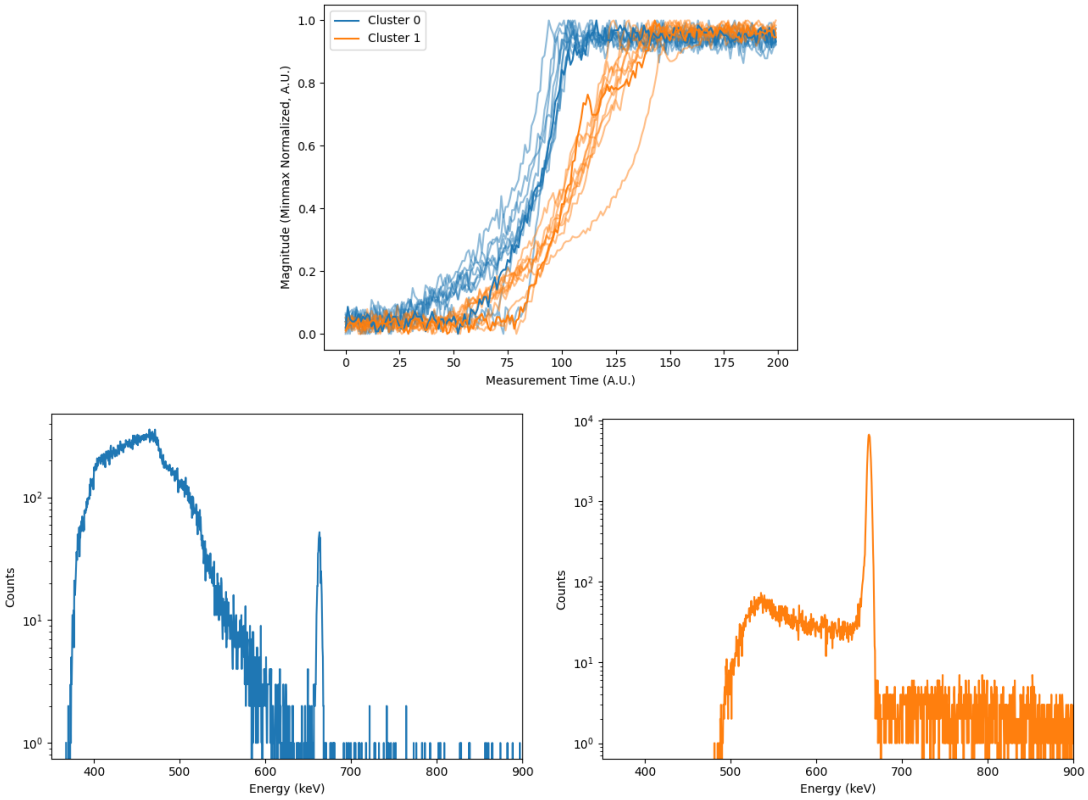

Figure 6: Result of k-means clustering algorithm with 3 output clusters.

Cluster	Number of Pulses	Mean Rise Time (ns)	PC Ratio	PT Ratio
0	46,249	219.1 +/- 0.4	0.96 +/- 0.43	0.006 +/- 0.021
1	79,281	224.7+/- 0.3	**inf**	**0.086 +/- 0.013**
2	26,527	244.0 +/- 0.5	8.81 +/- 0.63	0.009 +/- 0.043
All Pulses	**150,612**	226.3 +/- 0.3	21.14 +/- 0.07	0.0445 +/- 0.015

Table 4: PC and PT ratio of k-means clustering algorithm with 3 output clusters.

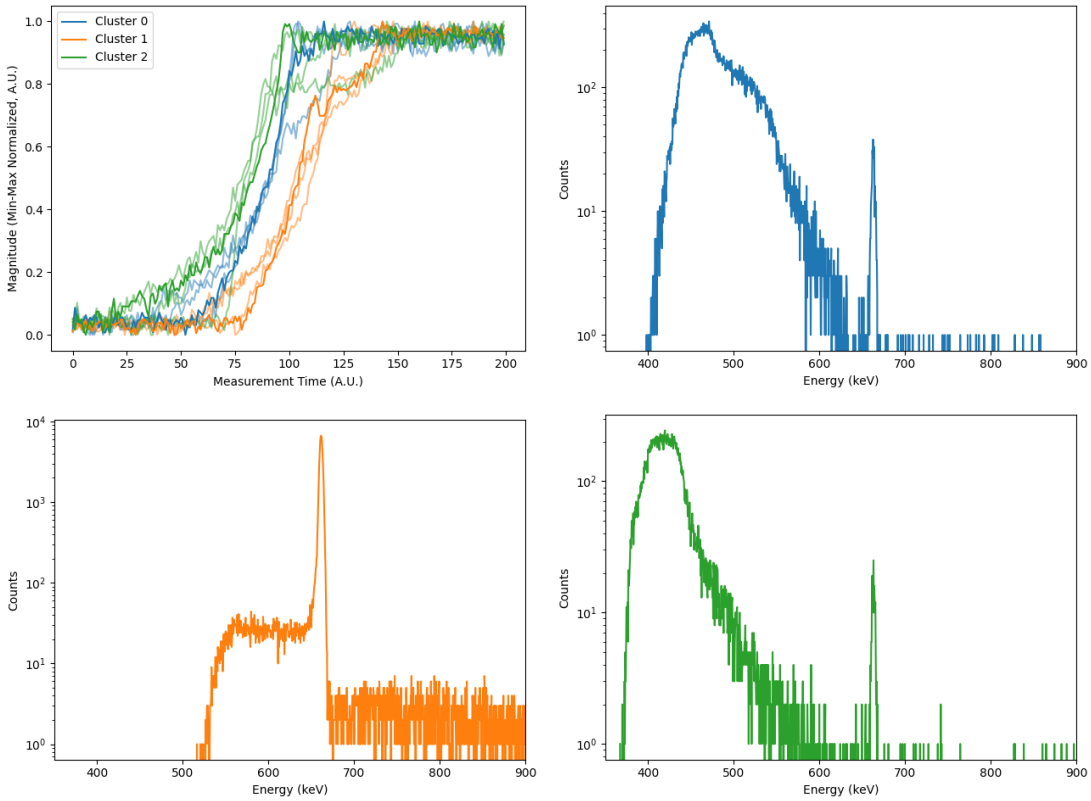

Figure 7: Result of k-means clustering algorithm with 3 output clusters.

Cluster	Number of Pulses	Mean Rise Time (ns)	PC Ratio	PT Ratio
0	77,480	224.8 +/- 0.3	**inf**	0.086 +/- 0.011
1	26,211	244.2 +/- 0.5	8.92 +/- 0.61	0.009 +/- 0.043
2	45,959	219.1 +/- 0.4	0.97 +/- 0.47	0.006 +/- 0.023
3	2,407	216.9 +/- 0.8	nan	0
All Pulses	**150,612**	226.3 +/- 0.3	21.14 +/- 0.07	0.0445 +/- 0.015

Table 5: PC and PT ratio of k-means clustering algorithm with 4 output clusters.

the presence of a Compton valley in the spectra. Cluster 3 consists only of events with energies above the photopeak channel. These events consist of a relatively small fraction of waveforms, and are likely due to multiple gamma-rays interacting in the detector at the same time.

Table 5 shows the mean rise time and spectral characteristics for each of the 4 clusters. As expected, cluster 0 has the the largest PT ratio and an incalculable PC ratio. The PC ratio for cluster 3 is also incalculable due to the fact that the lowest energy event in the cluster is greater than 800 keV. The PT ratio is 0 because there are no 662 keV photopeak counts present.

5 clusters

The final clustering filter used divides the waveforms into five clusters. Fig. 9 shows the 5 typical pulse shapes and spectra for each of the 5 clusters. We see that the spectra are similar to those obtained by the filter with 4 clusters; however, these results show two spectra (cluster 1 and 3) which have a high photopeak with a suppressed Compton continuum. The differences in these two clusters could be that one cluster is comprised of multi-interaction full-energy events. Table 6 shows the mean rise time, PC ratio, and PT ratio of the five clusters.

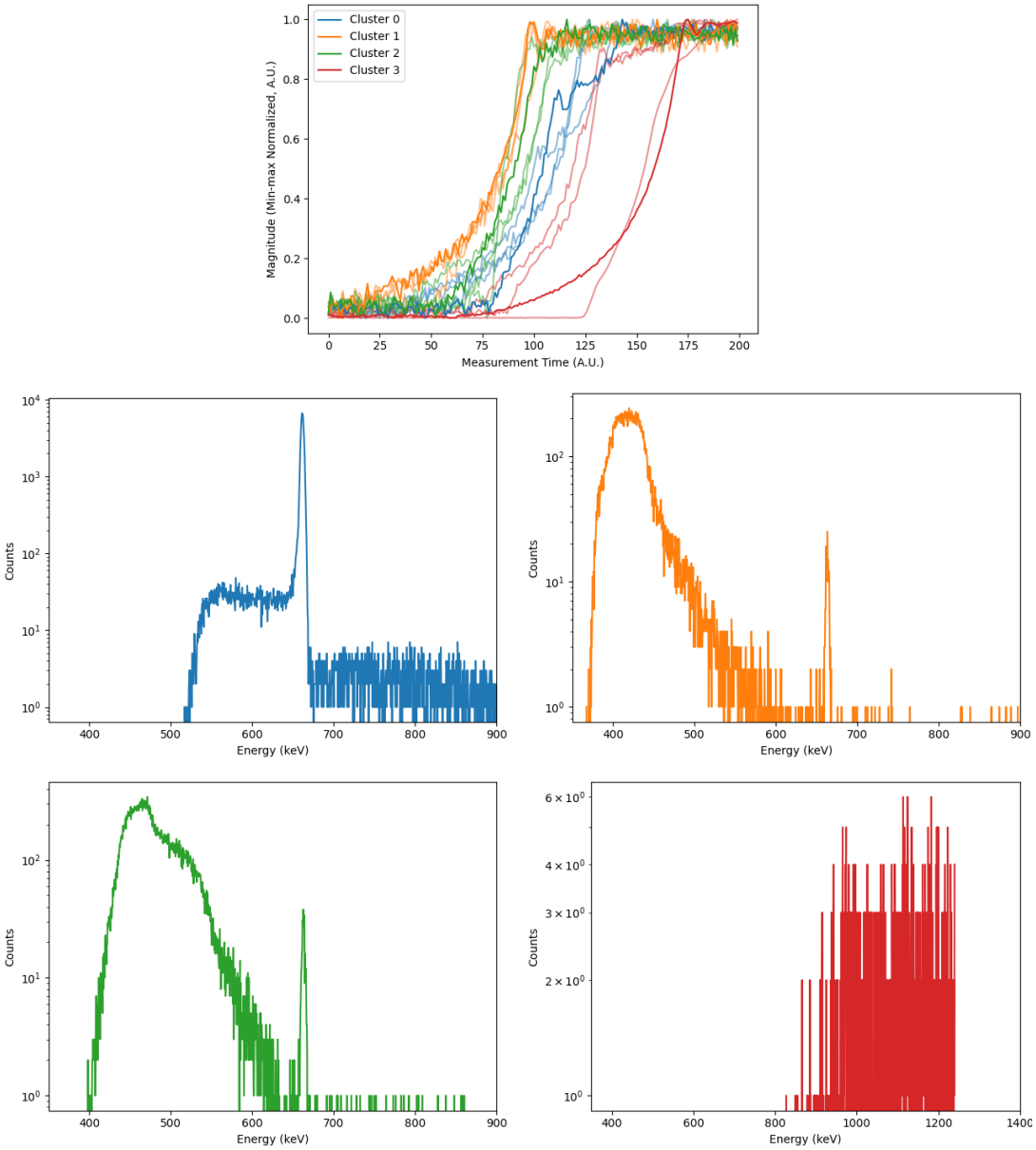

Figure 8: Result of k-means clustering algorithm with 4 output clusters. Note the change in energy scale for Cluster 3.

Cluster	Number of Pulses	Mean Rise Time (ns)	PC Ratio	PT Ratio
0	26,174	244.2 +/- 0.5	8.889 +/- 0.63	0.009 +/- 0.045
1	19,906	288.3 +/- 0.6	**inf**	0.084 +/- 0.039
2	45,415	217.6 +/- 0.4	0.971	0.006 +/- 0.024
3	58,161	204.3 +/- 0.4	**inf**	**0.087 +/- 0.029**
4	2,401	216.7 +/- 0.8	nan	0
All Pulses	**150,612**	226.3 +/- 0.3	21.14 +/- 0.07	0.0445 +/- 0.015

Table 6: PC and PT ratio of k-means clustering algorithm with 5 output clusters.

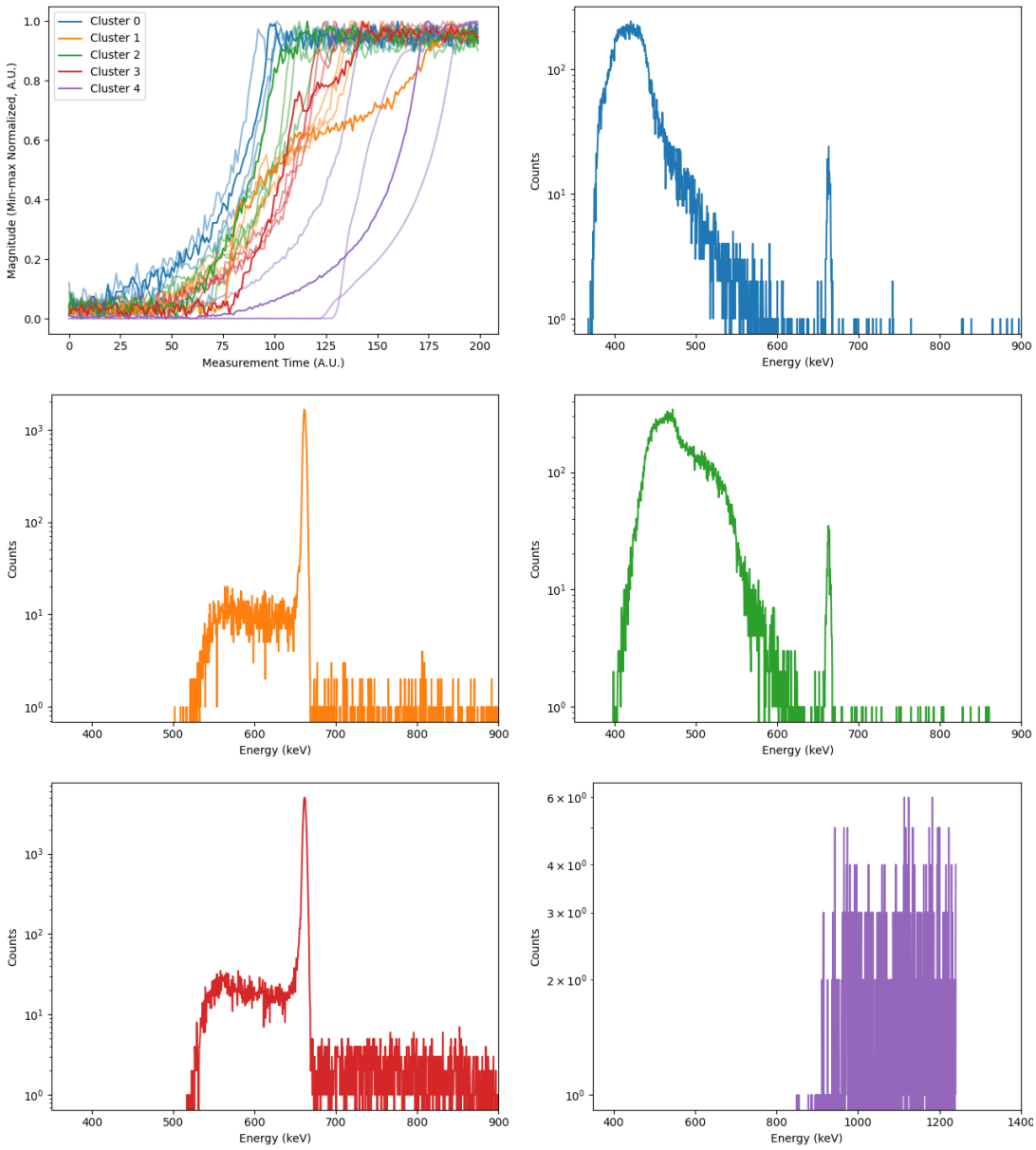

Figure 9: Result of k-means clustering algorithm with 5 output clusters. Note the change in energy scale for Cluster 4.

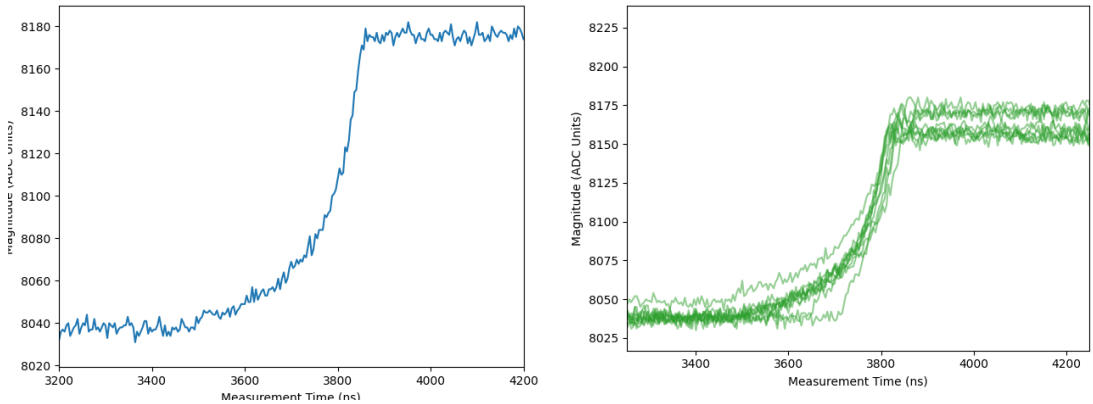

Figure 10: Left: Pulse sampled from Compton Valley , Right: Random sample of 10 pulses from cluster 2 of k-means clustering algorithm with 4 output clusters

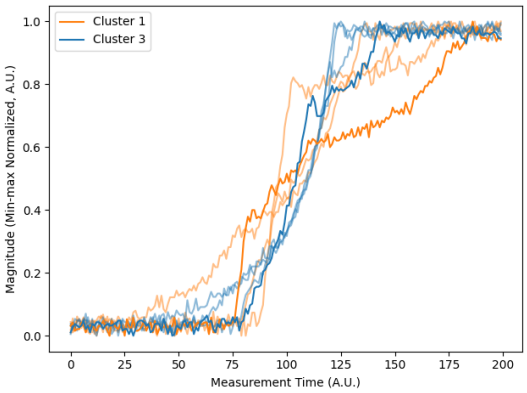

Figure 11: Peak shapes of cluster 1 and 3 from k-means clustering algorithm with 5 output clusters

0.9 Multi Interaction Events

For a Cs-137 spectrum where only single interaction events occurred, we would expect to see a peak at 662 keV representing full energy deposition events and a Compton continuum between the Compton backscatter peak and Compton edge. We know that these pulses are results of multiple interaction events, so we can investigate their pulse shapes. Fig. 10 left shows an example pulse from the Compton valley region of the spectrum. The mean rise time of the pulses in the compton shoulder region is 234.8 ns while the rise time of the pulse shown is 244 ns. Fig. 10 right shows a sample of pulses from cluster 2 in Fig. 8. The mean rise time for this cluster is 219.1 +/- 0.4 ns.

It is also possible to have multiple interaction events in the photopeak. For the k-means clustering algorithm with 5 clusters, two clusters that are predominately photopeak events were identified. It could be that the difference in pulse shapes between these two clusters is that one is comprised of multiple interaction events, while the other is comprised of single interaction events. Fig. 11 shows typical pulse shapes of these two clusters. The general shapes of these pulses, as well as the mean rise time from Table 6, show that the rise time is longer for cluster 1 and shorter for cluster 3. Assuming that these are all photopeak events, the cluster with the longer rise time (cluster 1) is likely composed of multi-interaction events.

Discussion

0.10 Conclusions

In this experiment, pulse shapes were analyzed to infer interaction history of the incident 662 keV gamma-rays. A series of event filters were devised to improve the PC and PT ratio of spectra. It was found that clustering algorithms perform the best in suppressing the Compton continuum in a spectrum. The clustering algorithms were also instructive in determining pulses which consist of multiple interaction events. In this experiment we only clustered the pulses into groups of 2, 3, 4, and 5, but higher numbers of clusters could be used to analyze more pulse behavior and further investigate interaction history. Additional analysis could include using a clustering algorithm to cluster waveforms with signals predicted by the Shockley-Ramo theorem, which could be used to estimate the radial position of the interactions in the detector.

References

[1] BeARING. *Ethernet Data Aquisition Code for SIS3316 250MHz Digitizers*. `https://github.com/bearing/python3316/tree/raw_waveform_fix_later`. 2021.

[2] Tadeusz Caliński and Harabasz JA. "A Dendrite Method for Cluster Analysis". In: *Communications in Statistics - Theory and Methods* 3 (Jan. 1974), pp. 1–27. DOI: `10.1080/03610927408827101`.

[3] National Nuclear Data Center. *NuDat 2.8*. `https://www.nndc.bnl.gov/nudat3/nudat2.jsp`. 1996.

[4] R Cooper. "Digital Gamma-Ray Spectroscopy: Trapezoidal Filtering". en. In: (2013), p. 4.

[5] Glenn F. Knoll. *Radiation detection and measurement*. en. 4th ed. OCLC: ocn612350364. Hoboken, N.J: John Wiley, 2010. ISBN: 978-0-470-13148-0.